PAPER

A New Scheme to Enhance Bandwidth of Printed Dipole for Wideband Applications

Dinh Thanh LE[†*a)], **Nguyen Quoc DINH**[††], ***Members***, ***and*** **Yoshio KARASAWA**[†], ***Fellow***

SUMMARY This paper presents a new technique to enhance the bandwidth of a printed dipole antenna for ultra-wideband applications. The basic idea is to exploit mutual coupling between the feeding line, which is designed closed and paralleled to dipole arms, the dipole arms and other elements of the antenna. Dipole arms, feeding lines as well as other parts are investigated in order to expand antenna bandwidth while still retaining antenna compactness. Based on the proposed technique, we develop two sample printed dipole antennas for advanced wireless communications. One is an ultra-wideband antenna which is suitable for multi-band-mode ultra-wideband applications or being a sensing antenna in cognitive radio. The other is a reconfigurable antenna which would be applicable for wideband cognitive radios. Antenna characteristics such as radiation patterns, current distributions, and gains at different frequencies are also investigated for both sample antennas.

key words: *printed antennas, dipole, mutual coupling, ultra-wideband antennas, reconfigurable antennas*

1. Introduction

The printed antenna, one of the most common types of antennas, has been developed over a long time. With a number of advantages, namely low cost, low profile or easy fabrication, they are increasingly utilized in many systems. However, a printed antenna, particularly a printed dipole, normally offers a narrow bandwidth [1], [2], thus making it difficult for it to support wideband applications. Much effort has been carried to enhance the bandwidth of printed antennas and a lot of techniques have been reported [3]. Thanks to these enhancements, many printed antennas can offer a relative bandwidth of up to 20%–40%. However, antennas with a wider bandwidth are still needed in many advanced wideband applications such as ultra-wideband (UWB) technology [4] or sensing antenna in cognitive radio [5].

Since the FCC (Federal Communications Commission) released commercial UWB bandwidth (from 3.1 to 10.6 GHz), wideband printed antennas have become the subject of more and more interest. As a result, a number of printed UWB antennas were introduced in last decade [6]–[17]. Most of these designs are based on tapered slot antennas [8], [9], planar slot antennas [10], or planar monopole antennas [11]–[16]. Only few designs are based on the dipole type, where the dipole arms were modified as a planar or a bridge. Nevertheless, a long balun microstrip may be required for impedance matching issue [17]. Therefore, these wideband printed dipole may be still complex and large.

In addition, when enhancing the bandwidth of a printed antenna, an engineer normally must address the trade-off with antenna size. In fact, the overall sizes of available UWB printed antennas are usually around 40 mm × 50 mm to 25 mm × 25 mm whereas, those of UWB printed dipoles are 40 mm × 18 mm (without a long-size balun) [17]. Therefore, designing a wideband and compact printed dipole would be a difficult work. To address this difficulty, we have introduced a simple design of wideband dipole for wideband MIMO cognitive radio application [18]. The proposed dipole offers a relative bandwidth of up to 50%, covering the range of 2.4 GHz to 4.0 GHz while its size does not exceed 15 mm × 80 mm.

In this paper, we present a new scheme to enhance bandwidth of a printed dipole, making it suitable for ultra-wideband applications [19], [20]. Based on the proposed scheme, an UWB dipole antenna and a reconfigurable dipole antenna are designed and fabricated as examples. The ultra-wideband dipole antenna offers a relative bandwidth of 95.5% for voltage standing wave ratio (VSWR) less than 2, extending from 3.5 GHz to more than 9.9 GHz. The reconfigurable antenna, on the other hand, can provide multiple wideband operation in two frequency ranges of 2.41 GHz to around 4 GHz, and around 4 GHz up to 6.88 GHz, offering a total relative bandwidth of 96.2%. Both sample antennas are designed in a compact size, only 9 mm × 57.5 mm for the UWB dipole antenna and 13.5 mm × 71 mm for the reconfigurable antenna. The two sample antennas emphasize the simplicity and usefulness of the proposed scheme to enhance bandwidth of printed dipoles for advanced wideband applications.

The rest of this paper is organized as follows. In Sect. 2, the principle scheme for enhancing bandwidth of a printed dipole is investigated. Two sample antenna designs, based on the proposed technique, are illustrated in Sect. 3 and Sect. 4 with detailed discussions. Some concluding remarks and next works will be presented in Sect. 5.

Manuscript received June 1, 2013.
Manuscript revised November 2, 2013.

[†]The authors are with the Advanced Wireless Communication research Center (AWCC), The University of Electro-Communications, Chofu-shi, 182-8585 Japan.

[††]The author is with the Faculty of Radio-Electronics, Le Quy Don Technical University, 100 Hoang Quoc Viet, Ha Noi, Vietnam.

[*]Presently, with Electromagnetic Compatibility Laboratory, National Institution of Information and Communication Technology, Koganei-shi, 184-8795, Japan.

a) E-mail: ledt@nict.go.jp

DOI: 10.1587/transcom.E97.B.773

Copyright © 2014 The Institute of Electronics, Information and Communication Engineers

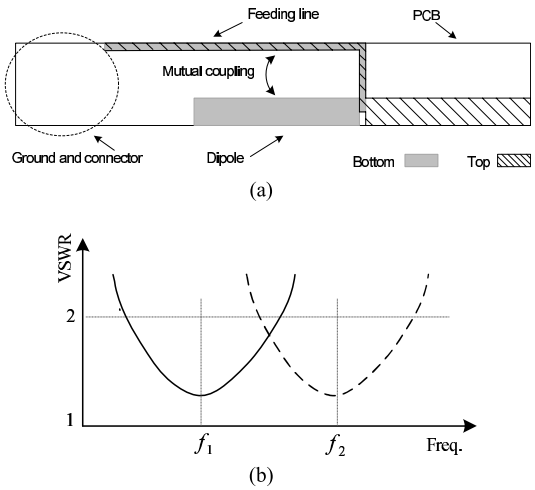

Fig. 1 Printed wideband dipole: (a) Fundamental structure; (b) Multiple resonance characteristic.

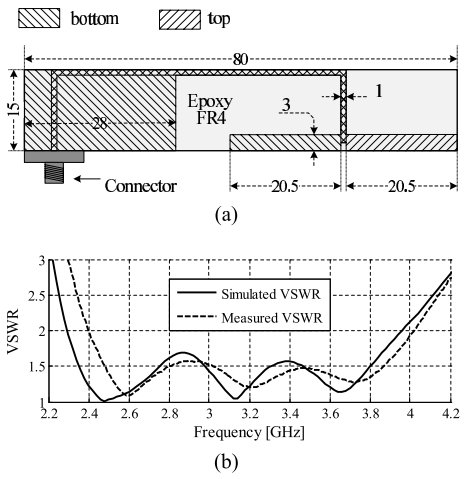

Fig. 2 Printed wideband dipole: (a) Antenna structure (all dimensions are in mm); (b) VSWR characteristics.

2. Fundamental Concept

In this work, we realize the possibility of exploiting mutual coupling between components of a printed dipole in order to expand its bandwidth while minimize its size. The arms of the dipole, as original design, are remained as thin and small as those of conventional printed dipoles. The main idea is to design a transmission feeding line that is closed and paralleled to the arms. The mutual coupling between the dipole arms and the transmission line will make the current distributions on the transmission line changed. In particular, the currents on the top and the bottom lines of the transmission line will be unbalanced. Therefore, even if the directions of the currents on the lines are opposite, but because they are not equal, the total electric field radiated from the lines will not be vanished. This means that the transmission line acts as an additional radiating element in a frequency region. Since the length of the dipole and the length of the transmission line are different, they resonate at different frequencies. The total combined performance of the dipole and the transmission line will create wide-band characteristic of the whole antenna.

2.1 Basic Technique

A fundamental structure between dipole and transmission feeding line is illustrated in Fig. 1(a). The dipole has two arms and the transmission line also has two lines laying at two sides (top and bottom as shown in the figure) of a printed circuit board (PCB). The transmission line connects to the dipole arms at respective sides to feed the dipole. Furthermore, a piece of ground and a connector can be added at the other end of the transmission line.

With a certain length of dipole arms corresponding to a certain resonated frequency, f_1, for example, the length of the transmission line as well as the distance between transmission line and dipole would affect directly to antenna bandwidth. Basically, there are two options for enhancing antenna bandwidth. Option one is to make the length of transmission line corresponding to lower frequency f_2, i.e. $f_2 < f_1$. The other option, in contrast, is to make the length of transmission line shorter, corresponding to higher frequency, i.e. $f_2 > f_1$. As a result, the bandwidth of the dipole will be expanded into lower band for the first option, while it will be expanded toward higher band for the second one.

Figure 1(b) shows the multiple resonance characteristic of the dipole and the transmission line for the case $f_2 > f_1$. At low frequency region, the main radiation is from the dipole, whereas at higher frequency range, thanks to mutual coupling between the dipole and the transmission line (and other parts of antennas such as ground), currents on the top-side line and bottom-side line of the transmission line will be unbalanced. Thus, the transmission line will act as an additional radiating source, creating multiple resonance characteristic. Combination performances of the dipole and the transmission line would result in expanding over all bandwidth of the antenna.

Figure 2 shows an example of a completed design and its VSWR characteristics as we introduced in [18]. In this design, the length of transmission line is longer compared with the length of dipole arms. The principle operation is just similar to the description above except, for this design, the transmission line will act as a radiation source, extending antenna bandwidth into lower frequency range (option one). At high frequencies, because the mutual coupling is relatively weak, the main radiation source would be the dipole only. This antenna offers a bandwidth of over 50% for VSWR less than 2 while still has radiation patterns similar to a conventional dipole.

2.2 Improvement

In order to achieve a wider bandwidth while minimizing antenna size, it would be also possible to design a short trans-

mission line connecting with a long-arm dipole. Combined performances of these components at different frequencies can also expand antenna bandwidth as mentioned in the second option in the previous section. The transmission line will act as a radiation part at high frequencies, while the dipole will cover the bandwidth at lower frequencies.

Furthermore, the shape of dipole arms, the connecting point to feeding source, and ground area may be also considered in design so that currents on the transmission line are more unbalanced. For example, instead of thin and straight lines, the dipole arms can be modified as the Vivaldi-type to inherit additional resonance and increase mutual coupling between the transmission line and the arms. This type of arms would also provide a wider bandwidth. However, it is noted that re-shaping the dipole arms would result in more complicated design since the conventional thin and straight arms are much simpler. An alternative way to enhance bandwidth of the antenna is to design the transmission line with a vertical deflection between lines. By doing so, currents on the lines are more unbalanced, thus making it radiates more energy.

In the following sections, we will introduce two sample applications of the proposed technique in designing antennas for different wireless communication systems. One is an ultra-wideband dipole antenna which is suitable for multi-band-mode ultra-wideband applications or for a sensing antenna in cognitive radio. The other is a reconfigurable antenna which is applicable for wideband cognitive radios. Antenna structures as well as their characteristics will be presented with detailed discussions.

3. Ultra-Wideband Antenna Design

3.1 Antenna Structure

This section presents an application of the proposed technique in designing an ultra-wideband dipole antenna. The configuration of the proposed antenna is illustrated in Fig. 3, and photographs on front and back views of a prototype antenna are shown in Fig. 4. The substrate material is the FR4 epoxy that has a relative permittivity of 4.4 and loss tangent of 0.02. The thickness of substrate is 1.6 mm.

Similar to the fundamental structure in Fig. 1(a), the antenna also consists of a dipole with thin and straight arms and a transmission line to feed the dipole. The arms of the dipole as well as two lines of the transmission line are assembled at different sides of the antenna substrate. Furthermore, to widen the bandwidth of the antenna into low frequencies, we extend the transmission line in the top side and connect it to a rectangular patch. Mutual coupling between the patch and the top-side arm of the dipole also plays an important role to force currents on the transmission line unbalanced. In addition, for further developments for some advanced systems, the patch area can be used to integrate another UWB antenna (a slot UWB antenna, for example) for UWB-MIMO applications or a communication antenna in cognitive radios.

In the simulation, the frequency dispersive property of FR4 has not been taken into account. The thickness of copper layer is simulated with value of 0.02 mm. The geometrical parameters, optimized to obtain the possible largest bandwidth for VSWR less than 2, are as following, $m = 10.5$ mm, $d1 = 8.5$ mm, $d2 = 21$ mm, $s1 = 3.5$ mm, $s2 = 3$ mm, $a = 0.5$ mm, $w = 2$ mm, $p = 4$ mm, $q = 1.5$ mm, and $n = 9$ mm.

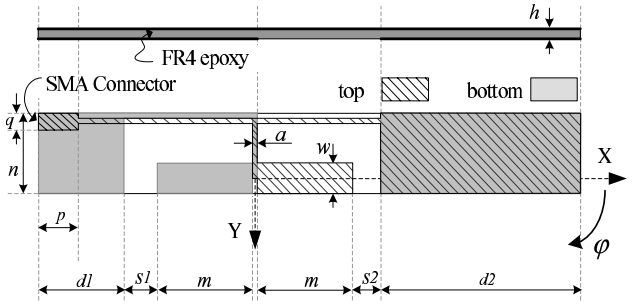

Fig. 3 Geometry of proposed ultra-wideband dipole antenna.

3.2 Parametric Study

In order to understand the operation of the proposed antenna, it is useful to investigate the performance of the antenna by changing its geometrical parameters. The effects of some key parameters will be explored by alternatively adjusting each parameter while keeping the others unchanged. To keep the paper concise, we will only present in this section parametric studies on length of dipole arm, width of antenna, and the length of patch as they may play important roles in expanding antenna bandwidth.

Dipole arm-Related (m): The dipole obviously plays an important role in the whole antenna performance. Thus, the impedance matching is very sensitive to its geometrical parameter. Among parameters of the dipole, we examine the variation of length of dipole arm as it would be the most important. Figure 5 shows the effect of varying the parameter on the impedance matching. At low frequency region of the antenna bandwidth, the dipole plays an important role in radiation. A longer length of dipole would result in extending bandwidth into lower frequency. In the meantime, the gap between dipole arm and the edge of the patch is shorter, thus enhancing mutual coupling between them. Thus, cur-

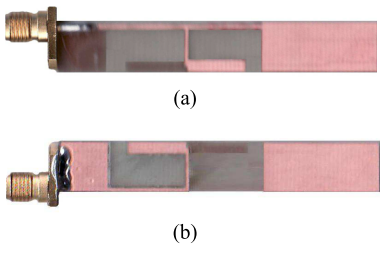

Fig. 4 Photograph of the fabricated antenna: (a) front view; (b) back view.

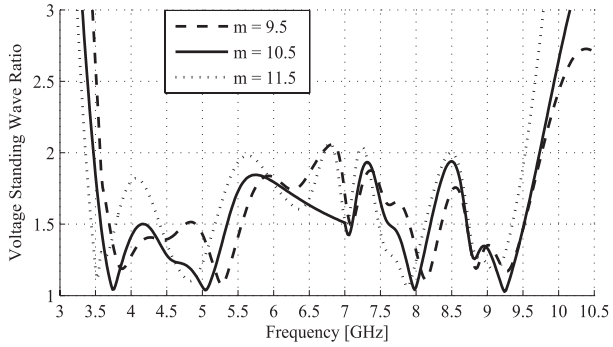

Fig. 5 Effects of varying length of dipole.

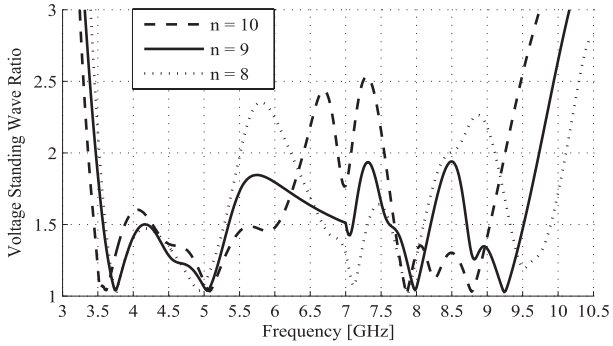

Fig. 6 Effects of varying width of substrate.

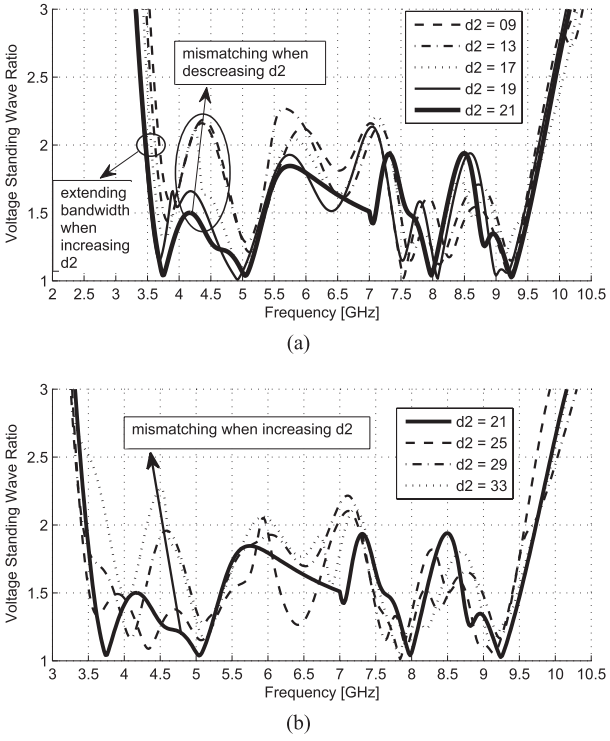

Fig. 7 Effects of varying length of loaded patch: (a) $d2 < 21$ mm; (b) $d2 > 21$ mm.

rents on transmission line, and currents on the short edge of the patch will be changed. As a result, antenna performance in high frequency (around 7.5 GHz) will be also changed.

Width of antenna-Related (n): When compared with other available printed UWB antennas [8]–[17], one of the advantage of this proposed antenna is the small dimension of substrate width. With this distinguished feature, the antenna can be easily integrated into a narrow space in portable devices. When designing the antenna, we tried to optimize it as small as possible.

Figure 6 illustrates the impact of width of substrate on the antenna operating bandwidth. In fact, this dimension has a critical effect on impedance matching of the antenna. The reason is because it directly relates to mutual coupling between the dipole and the transmission line, which both are very important in antenna operation. In particular, since n represents to the distance between the dipole and the transmission line, the currents on transmission lines will be changed directly when n is changed. With an optimized value of n, good impedance matching can be observed over the whole bandwidth of the antenna. In the meantime, the transmission line acts as a radiating component, extending the bandwidth of the dipole into higher frequency region. The combined performance of the dipole, the transmission line, and the other elements (including transmission line and the patch) will create the wide-band characteristic of the whole antenna.

Since impedance matching of the antenna is much sensitive on mutual coupling between components of the antenna, the variation of width of substrate will significantly result in changing resonance frequency, particularly in high frequency region. For instance, as shown in Fig. 6, when n equals to 8 mm or 10 mm, some different resonating frequencies occurred (around 7 GHz to 9.5 GHz). Also, the impedance matching may become a serious issue in the high frequency region. To achieve good impedance matching over a wide band, the value n of 9 mm is chosen in the final design.

Length of patch-Related (d2): Simulated data for $d2$ are shown in the Fig. 7 for both cases: less than, and greater than a local optimized value of 21 mm. From the Fig. 7(a), we can see that when the length of $d2$ is increased (but still less than 21 mm), the bandwidth of antenna is extended into lower frequency, thus widening the bandwidth. However, when $d2$ exceeds the optimized value, increasing $d2$ will result in mismatching problem as shown in Fig. 7(b). In both cases, when $d2$ is longer or shorter than 21 mm, mismatching around 4.5 GHz can be witnessed. We can expect that performances of the dipole and the patch together create multiple resonance characteristic at the low frequency region of the bandwidth.

There are two important issues those need to be considered when increasing length of $d2$. First, the total size of the antenna will be increased, thus losing the compactness of the antenna. Second, as mentioned above, currents of the top-side of the transmission line will be changed. This will affect on the performance of both the dipole and the patch. To achieve good matching and remaining the compactness

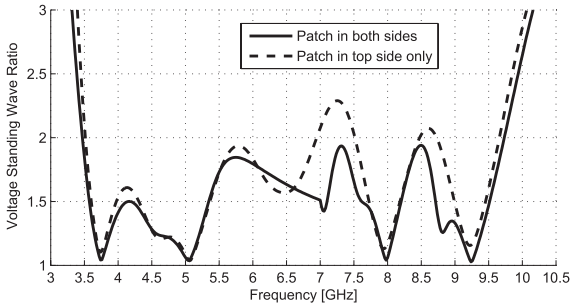

Fig. 8 VSWR with/without the bottom patch.

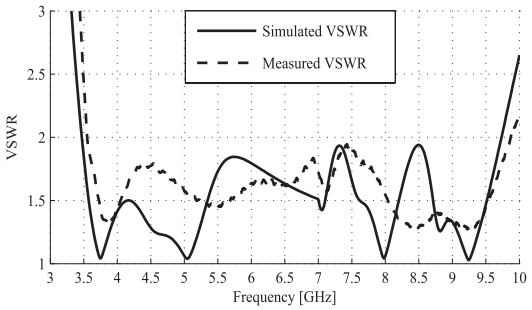

Fig. 9 Measured and simulated VSWR of the proposed antenna.

of the antenna, the value $d2$ of 21 mm is chosen.

Patch design-Related: Compared to the fundamental design in Fig. 1, we added the patch at the end of the transmission line and closed to the top-side arm of the dipole to enhance the bandwidth of the dipole in this design. The patch, in fact, can be designed with the top-element only. Such structure can also support wideband characteristic as shown in Fig. 8. Optimizations may be necessary to obtain good matching in this case. However, for further studies on UWB-MIMO applications, we intentionally design the patch in both top and bottom sides so that another antenna (tapered-slot antenna, for example) can be integrated in this area. By doing so, we may achieve a dual-polarization two-port UWB-MIMO antenna in a compact size. Since the patch is quite small, realizing the integrated antenna for such UWB-MIMO antenna would be a challenging work.

From the principle parametric studies above, we can see that the antenna may have more than two resonances those are described in Fig. 1(b). The reason is because the fundamental structure in Fig. 1(a) only consists of two basic elements: the dipole and the transmission line, while the improvement design in the UWB antennas has additional elements such as the patch and the top-side segment of the transmission line connecting to the patch. Radiating elements corresponding to resonance frequency regions can be approximated as following: the patch is for frequencies around 3.5 GHz and lower; the dipole is for frequencies around 4 GHz to 6 GHz; the segments of the top line of the transmission and the short edge of the patch are for frequencies around 6.5 GHz to 7.5 GHz, and the transmission line is for the band around 7.5 GHz to 9.7 GHz. Since the elements are electrically related, it is not simple to clearly clarify individual resonating bands of them. The performance of the whole antenna is the combined performance of all elements.

3.3 Antenna Characteristics

We measured a fabricated ultra-wideband dipole antenna by a vector network analyzer in an anechoic chamber. Figure 9 shows the comparison of the simulated and measured VSWR characteristics of the antenna. As can be seen from this figure, the measured bandwidth, for VSWR less than 2, covers the range of 3.5 GHz to 9.9 GHz, accounting for a relative bandwidth of over 95.5%. The VSWR response across the bandwidth features a multiple resonance operation. Also, simulation and measurement are in good agreement.

It is noted that, in simulation, the simulated excitation source with a 50 Ω internal resistance is placed between the end of the feeding strip and the grounding plane. SMA connector and RF cable have not been considered in simulation. On the other hand, in measurement, the antenna is fed by the VNA via an FR cable and an SNA connector. Even so, good agreement between simulation and measurement can be seen in Fig. 9. Thus, we may expect that leaky currents on the coaxial cable would be small and does not affect to the antenna performance. This feature emphasizes that the proposed antenna can be easily integrated into a small device for a real application without a serious consideration on the impedance matching issue.

Figure 10 illustrates the measured radiation patterns at different frequencies in both E plane and H plane. As can be seen from this figure, in the low frequency region, antenna radiation pattern is similar to that of a dipole, whereas in the high frequency region, there are some additional beams. This confirms that at the low frequencies, the dipole plays a significant role in antenna performance, while at high frequencies, a combination of radiation components plays the main role in radiating energy. The combination may also make the antenna patterns distorted.

Figure 11 shows the peak gain of the antenna in E-plane for both simulation and measurement results. The peak gain is determined as the maximum gain in the plane without considering to any specified direction. As can be seen from the figure, the antenna offers good gains in the whole bandwidth. Measured peak gain varies from about 1.4 dBi to 5.2 dBi, making it comparable to the gain of a conventional half-wave dipole. The maximum measured gain can be achieved at frequency 6.36 GHz. Also, good agreement between simulation and measurement gains can be witnessed. Thanks to this good agreement, we may, again, expect that leaky currents on the coaxial cable may not affect much on the antenna performances even the ground is relatively small.

Considering about the direction of peak gain, we found that the peak gain directions in different frequencies are concentrated around 90∼100 degree. For instant, direction of the measured peak gain at 3.5 GHz, 6.0 GHz, 8.0 GHz,

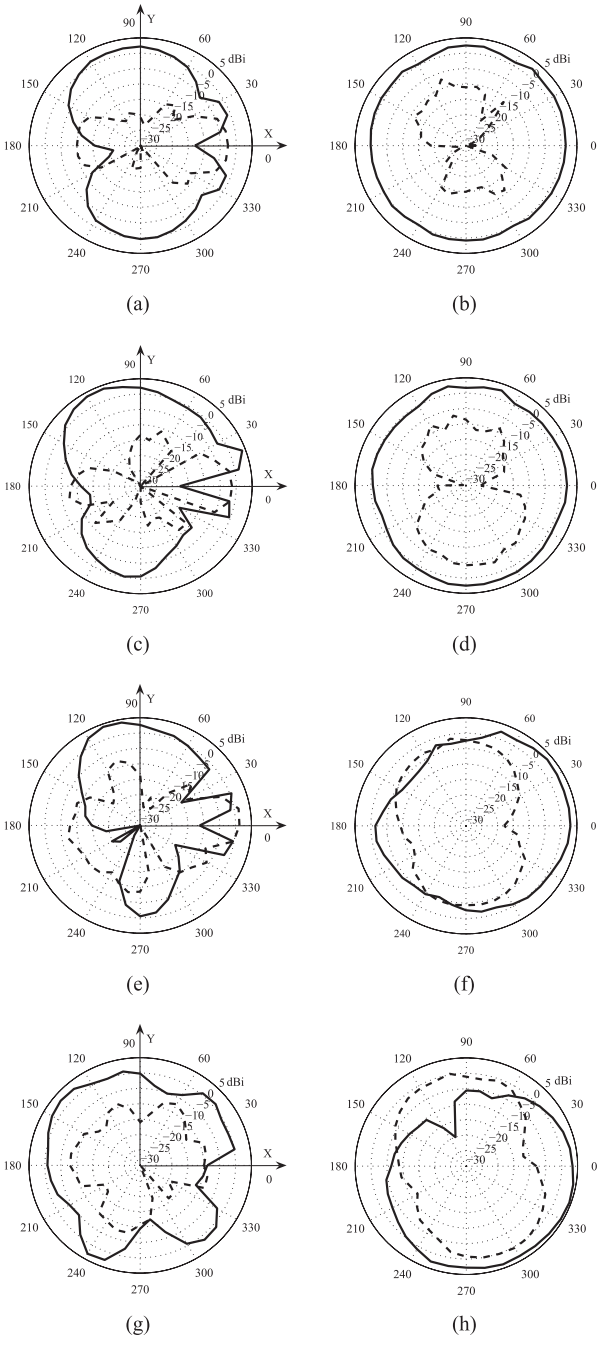

Fig. 10 Measured co-polarization (solid line) and cross-polarization (dashed line) radiation patterns of the antenna: (a) E-plane 3.5 GHz; (b) H-plane 3.5 GHz; (c) E-plane 5.5 GHz; (d) H-plane 5.5 GHz; (e) E-plane 7.5 GHz; (f) H-plane 7.5 GHz; (g) E-plane 9.7 GHz; (h) H-plane 9.7 GHz.

9.0 GHz, and 9.5 GHz is 90 degree, 110 degree, 110 degree, 150 degree, and 140 degree, respectively. At high frequencies, the pattern is distorted as shown in Fig. 10, thus the direction of peak gain is far from 90 degree as it is original peak gain direction of a conventional half-wave length dipole.

In order to provide an insight view of antenna performance, we explore the current distributions in simulation

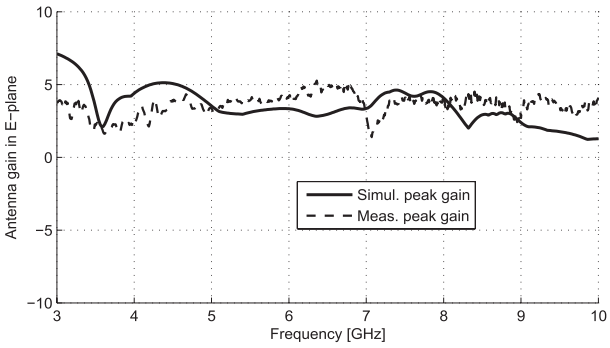

Fig. 11 Peak gain of the UWB antenna [dBi] in XY plane.

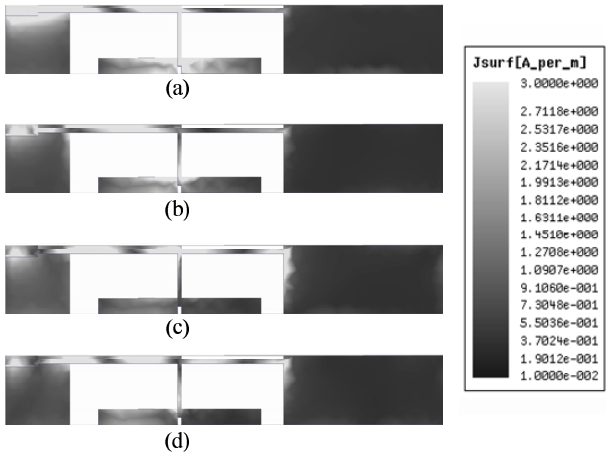

Fig. 12 Simulated current distribution (brighter color corresponds to higher value): (a) 3.5 GHz; (b) 5.5 GHz; (c) 7.5 GHz; (d) 9.7 GHz

at some different frequencies as shown in Fig. 12. At the low frequency region of the antenna bandwidth (around 3.5 GHz), the main radiation part is the dipole since electric currents on it are strong compared with currents on other parts. As a result, radiation pattern is similar to that of a conventional dipole as shown in Figs. 10(a) and 10(c). However, there are still some side lobes, mainly due to the effects of the transmission lines and the SMA connector of the antenna.

On the other hand, at high frequency region shown in Figs. 12(c) and 12(d), currents on the dipole and the patch are relatively weak whereas a majority of the electric currents is concentrated on the transmission line. Thanks to the unbalanced design of transmission line as well as mutual coupling between the dipole, the patch and the transmission line, the transmission line will act as a radiation part. It is also noted that the upper line of the transmission line consists of two segments separated by the feeding line of the dipole. These segments and the short edge of the patch correspond to multiple resonance operation at the high frequency region.

In comparison with the current distributions of the basic broadband antenna in [18], there are two important differences. First, at lower frequencies, currents on the dipole in [18] are weaker, whereas currents on the dipole in the

UWB antenna in this paper are stronger. On the other hand, at higher frequencies, currents on transmission line in [18] are weaker, while currents on the transmission line and the short edge of the patch in this paper are stronger. The reason is because these two antennas are based on two different options discussed in Sect. 2.1. In [18], the length of transmission line is longer than the length of dipole (option 1), whereas in this paper, the length of transmission line of the proposed UWB antenna is shorter than the length of the dipole (option 2). Therefore, in [18], the transmission line is the main radiating element in low frequency region, and the dipole is the main radiating element in high frequency region. In contrast, in this paper, the transmission line is the main radiating element in high frequency region, and the dipole is the main radiating element in low frequency region.

The second difference comes from multiple resonances thanks to the patch and the segments of transmission line on the top side. As shown in the Figs. 12(c) and 12(d), relatively strong currents on the short edge of the patch, where the patch connects to the top-side of the transmission line, indicates that additional resonances can be obtained at high frequencies. The patch, on the other hand, was not included in design in [18]. Thanks to shorter length of the transmission line in the scheme in this paper, the UWB antenna remains its compactness while still offers wide-band characteristics.

4. Reconfigurable Wideband Antenna Design

4.1 Antenna Structure

In this section, we will present another application of the proposed technique in designing of a reconfigurable dipole antenna for wideband cognitive radio. Figure 13 illustrates the structure of the dipole antenna. There are two branches which are connected to a shared ground (bottom side) and feeding strip (top side) by switches. Each branch has its own transmission lines and dipole. The long branch (on the right of the ground piece) is connected to the ground and feeding strip by switches 1 and 2. The short branch (on the left of the ground piece) is connected to the ground and feeding strip by switches 3 and 4. Switches 1 and 3 are on the top side, whereas switches 2 and 4 are on the bottom side of the antenna. The structure is similar to the fundamental one in Fig. 1(a), except there are additional switches to reconfigure the antenna. The substrate material, as well as its thickness, is similar to those of the ultra-wideband printed antenna in Sect. 3. Photographs on front and back views of a fabricated prototype (without integrated switches) are shown in Fig. 14.

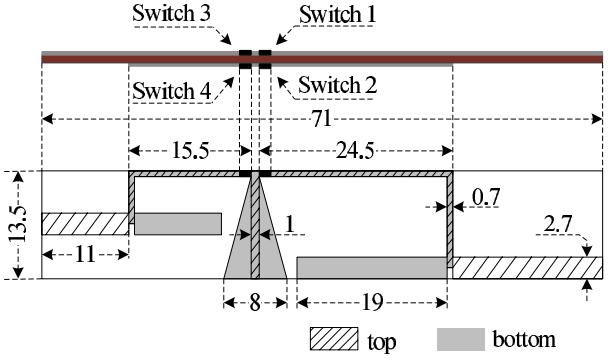

Fig. 13 Configuration of proposed reconfigurable antenna. All dimensions are in mm.

Basically, by setting switch pairs (1, 2) and (3, 4) alternatively ON or OFF the left or the right branch will be connected to the ground (on the bottom) and the feeding strip (on the top). When connected to the feeding strip by the switches, each branch will operate as a wideband antenna, which has input impedance of 50 Ohms. Because the reconfigurable antenna introduced in this section is to show an example application of the main technique discussed in Sect. 2, we will not focus on analyzing the performances of the switches. Principally, the switches are utilized to reconfigure the antenna, and we assume that their responds are ideal. However, when fabricating the antenna with real diode switches, one may need to consider on several issues such as respond duration of the switches, or the failure of switching those are discussed in [21], [22].

In addition, similar to the ultra-wideband dipole antenna design in the previous section, to retain antenna compactness, in each branch, the length of transmission line is relatively shorter than the length of dipole. It means that the transmission lines will correspond to the high frequency region, whereas the dipole corresponds to the low frequency region of the bandwidth of the branches.

Because the dimensions of each branch in Fig. 13 are in different scales, these branches will offer different bandwidths when they are connected to the feeding strip and the ground plane. Thus, the frequency reconfigurability can be achieved by just controlling switching pairs (1, 2) and (3, 4). Nevertheless, by setting some other combinations of these four switches, currents on each branch will be changed. Thanks to this change, radiation pattern of the antenna will also change. Therefore, pattern reconfigurability may be also obtained at some frequencies.

4.2 Results and Discussion

There are two bands for wideband frequency reconfigurability. The low band corresponds to states of switches 1 and 2 are ON. The high band, on the other hand, corresponds to states that switches 3 and 4 are ON. In each band, there are four other possible cases when other switches of the band

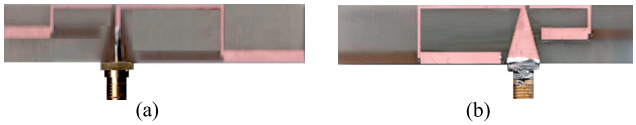

Fig. 14 Photograph of a fabricated prototype: (a) front view; (b) back view.

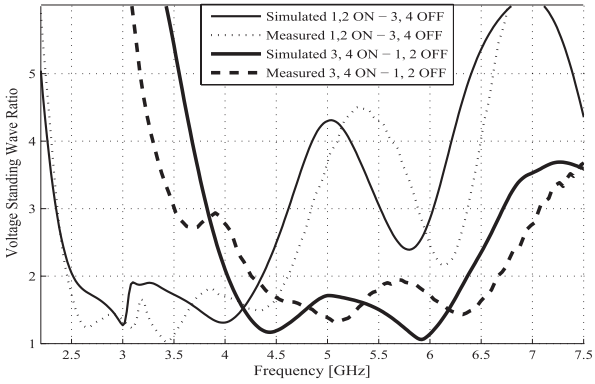

Fig. 15 VSWR vs. frequency when switches are ON/OFF.

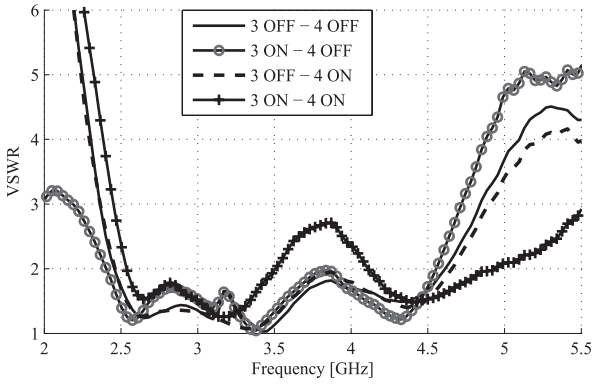

Fig. 16 Measured VSWR for low band (switches 1, 2 ON).

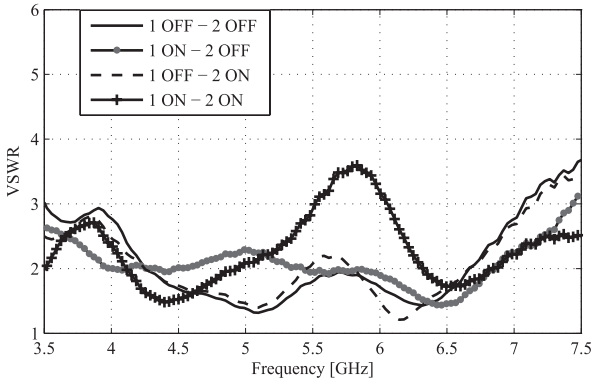

Fig. 17 Measured VSWR for high band (switches 3, 4 ON).

are ON or OFF. Figure 15 shows the comparison of the simulated and measured the VSWR of the antenna for the two bands. The measured bandwidth, for VSWRs less than 2, covers a range of 2.46 GHz–4.64 GHz for the first band, whereas for the second band, the antenna offers a bandwidth in a frequency range of 4.23 GHz–6.65 GHz.

Figures 16 and 17 show the measured VSWR for all possible state combinations of the switches which can offer wideband feature. The simulated and measured results are presented in Table 1. As can be seen from the table, the antenna can offer a wide bandwidth or multiple bands with different combinations of switch state. Also, good agreements between simulation and measurement can be witnessed for all the reserved combinations.

Table 1 Operating bands achieved when switches are ON/OFF.

Switch 1	Switch 2	Switch 3	Switch 4	Freq. band (GHz) Simulated (Measured)
ON	ON	ON	ON	2.50 ~ 3.40 (2.51 ~ 3.50)
				3.81 ~ 5.32 (4.08 ~ 4.99)
ON	ON	ON	OFF	2.49 ~ 4.26 (2.41 ~ 4.57)
				5.90 ~ 6.25 (6.14 ~ 6.49)
ON	ON	OFF	ON	2.49 ~ 4.36 (2.45 ~ 4.67)
ON	ON	OFF	OFF	2.50 ~ 4.38 (2.46 ~ 4.64)
ON	OFF	ON	ON	3.79 ~ 6.71 (3.97 ~ 6.88)
OFF	ON	ON	ON	3.82 ~ 6.38 (4.22 ~ 6.67)
OFF	OFF	ON	ON	4.06 ~ 6.36 (4.23 ~ 6.65)

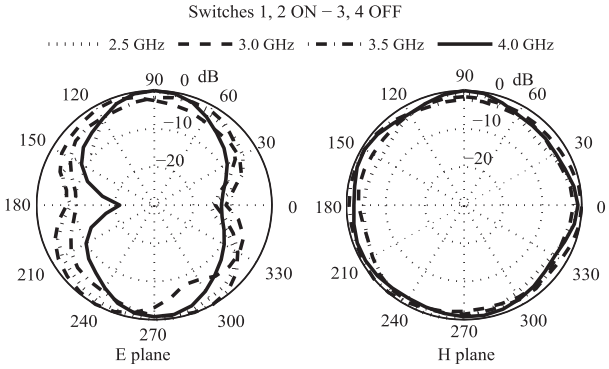

Fig. 18 Normalized gain patterns of the antenna.

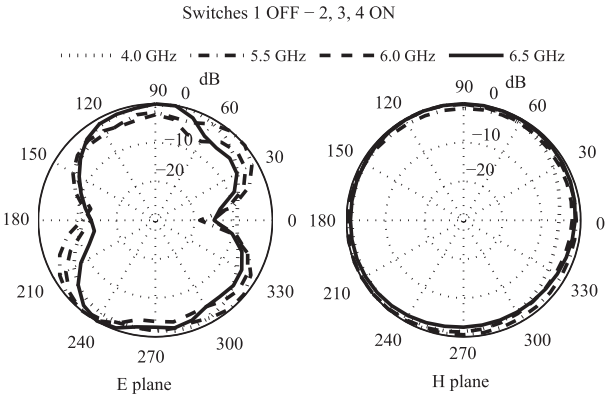

Fig. 19 Normalized gain patterns of the antenna.

In addition, for a same combination of switch states, when achieving good impedance matching in a wide frequency range, antenna should also have radiation pattern stability. Thus, examination on radiation patterns would be necessary. Figures 18 and 19 show the normalized simulated patterns of the antenna at different frequencies in both E plane and H plane in two typical combinations of switches. Data were normalized to the maximum gain among different frequencies in the same plane. For example, in Fig. 18, the gains of the antenna in the E plane for different frequen-

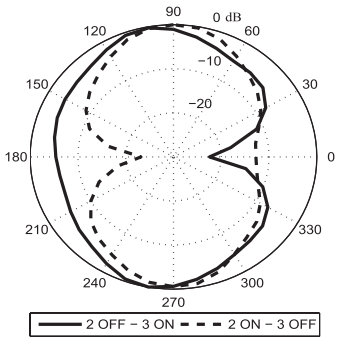

Fig. 20 Normalized gain patterns of the antenna at 4.0 GHz for two cases with switches 1, 4 ON.

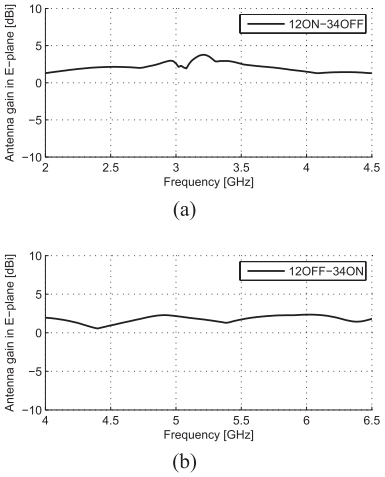

Fig. 21 Peak gain in E-plane: (a) Low band for switch combination 12ON-34OFF; (b) High band for switch combination 12OFF-34ON.

cies were normalized to the maximum of them. Thus, 0 dB indicates the frequency and the direction that has maximum gain. As can be seen from these figures, the radiation patterns keep mostly unchanged in a whole operating band.

Table 1 shows that some resonated frequencies can be achieved from different switch state combinations. For example, to operate at the frequency of 4.0 GHz, two possible switch combinations are switches (1, 2, 4) ON-3 OFF, and switches (1, 3, 4) ON-2 OFF. In such combinations, currents on the branches would be different due to different reconfigured structures. Therefore, although antenna may work at a same frequency, the radiation pattern of the antenna may be changed. As a result, radiation pattern reconfigurability may be achieved. Figure 20 shows the changes in radiation patterns at frequency of 4 GHz for the different switch state combinations. Data were also normalized to the maximum gain of them. Thanks to the changes, main lobes of antenna patterns are directed into different angles, making the antenna flexible in cognitive radio operations.

Figure 21 shows the simulated peak gain of the antenna in E-plane, including the switch combinations (1, 2) ON-(3, 4) OFF for low band and the switch combinations (1, 2) OFF-(3, 4) ON for high band. The peak gain at a frequency was determined by taking the highest gain among different directions. We can see that the gain of the reconfigurable antenna, in any band, is comparable to that of a conventional half-wave length dipole.

5. Conclusion

This paper presents a new scheme to enhance the bandwidth of the printed dipole antenna to suit wideband applications. Based on the scheme, we introduced two sample wideband printed dipole antennas. One is an ultra-wideband printed dipole. The other is a reconfigurable dipole. The first antenna offers a relative bandwidth of over 95.5% for voltage standing wave ratio less than 2, extending from 3.5 GHz to more than 9.9 GHz. The other can provide multiple wideband operation, covering a frequency range from 2.41 GHz to about 6.88 GHz. The designs of both antennas permit compact realization, making them realizable in a small volume. Characteristics of proposed antennas such as radiation patterns, gains, reconfigurability are carefully investigated. Measured and simulated results show that they would be suitable for wideband applications. In particular, the ultra-wideband dipole antenna would be applicable for multiband orthogonal frequency-division multiplexing or being a sensing antenna to sense environment in cognitive radio, whereas the reconfigurable antenna would be suitable to utilize in wideband reconfigurable antenna applications. Moreover, the structures of these antennas confirm that the proposed technique to enhance bandwidth of printed dipoles is simple yet very useful in designing antennas for wideband applications.

In the next step of this research, it would be also interesting to focus on integrating another UWB antenna into the ultra-wideband dipole antenna to realize an UWB-MIMO antenna, or to combine the two sample antennas to complete a set of sensing and communicating antennas for cognitive radios.

Acknowledgment

This research is funded by Vietnam National Foundation for Science and Technology Development (NAFOSTED) under grant number 102.01-2012.19. The authors are grateful to Prof. Nobuo Nakajima and Prof. Akira Saitou in AWCC (UEC-Tokyo) for their invaluable supports in manufacturing and measuring antennas, and Prof. Christos Christodoulou in University of New Mexico, US, for many helpful discussions.

References

[1] C.A. Balanis, Antenna theory analysis & Design, 2nd ed., John Wiley & Sons, NewYork, 1997.
[2] R. Garg, P. Bhartia, I. Bahl, and A. Ittipiboon, Microstrip antenna design handbook, Artech. House, Norwood, MA, 2001.
[3] D. Guha, "Broadband design of mirostrip antennas: Recent trends and developments," Mechanics, Autodmatic Control and Robotics, vol.3, no.15, pp.1083–1088, 2003.

[4] Z.N. Chen, "UWB antennas: Design and application," Proc. 6th Int. Conf. on Info. Comm. & Signal Proc, pp.1–5, Dec. 2007.
[5] C.G. Christodoulou, Y. Tawk, S.A. Lane, and S.R. Erwin, "Reconfigurable antennas for wireless and space applications," Proc. IEEE, vol.100, no.7, pp.2250–2261, July 2012.
[6] G. Adamiuk, T. Zwick, and W. Wiesbeck, "UWB antennas for communication systems," Proc. IEEE, vol.100, no.7, pp.2308–2321, July 2012.
[7] H. Nakano and J. Yamauchi, "Printed slot and wire antennas: A review," Proc. IEEE, vol.100, no.7, pp.2158–2168, July 2012.
[8] Z.-A. Zheng, Q.-X. Chu, and Z.-H. Tu, "Compact band-rejected ultrawideband slot antennas inserting with $\lambda/2$ and $\lambda/4$ resonators," IEEE Trans. Antennas Propag., vol.59, no.2, pp.390–397, Feb. 2011.
[9] G. Adamiuk, T. Zwick, and W. Wiesbeck, "Compact, dual-polarized UWB-antenna, embedded in a dielectric," IEEE Trans. Antennas Propag., vol.58, no.2, pp.279–286, Feb. 2010.
[10] A. Mehdipour, K.M. Aghdam, R.F. Dana, and M.R.K. Khatib, "A novel coplanar waveguide-fed slot antenna for ultrawideband applications," IEEE Trans. Antennas Propag., vol.56, no.12, pp.3857–3862, Dec. 2008.
[11] Z.N. Chen, T.S.P. See, and X. Qing, "Small printed ultrawide-band antenna with reduced ground plane effect," IEEE Trans. Antennas Propag., vol.55, no.2, pp.383–388, Feb. 2007.
[12] M. John and M.J. Ammann, "Antenna optimization with a computationally efficient multi objective evolutionary algorithm," IEEE Trans. Antennas Propag., vol.57, no.1, pp.260–263, Jan. 2009.
[13] Y.J. Cho, K.H. Kim, D.H. Choi, S.S. Lee, and S.-O. Park, "A miniature UWB planar monopole antenna with 5-GHz band-rejection filter and the time-domain characteristics," IEEE Trans. Antennas Propag., vol.54, no.5, pp.1453–1460, May 2006.
[14] L.-X. Li, S.-S. Zhong, and M.-H. Chen, "Compact band-notched ultra-wideband antenna using defected ground structure," Microwave Opt. Technol. Lett., vol.52, pp.286–289, Feb. 2010.
[15] M.E. Bialkowski and A.M. Abbosh, "Design of UWB planar antenna with improved cut-off at the out-of-band frequencies," IEEE Antennas Wireless Propag. Lett., vol.7, pp.408–410, Nov. 2008.
[16] W.T. Li, X.W. Shi, and Y.Q. Hei, "Novel planar UWB monopole antenna with triple band-notched characteristics," IEEE Antennas Wireless Propag. Lett., vol.8, pp.1094–1098, 2009.
[17] X.N. Low, Z.N. Chen, and T.S.P. See, "A UWB dipole antenna with enhanced impedance and gain performance," IEEE Trans. Antennas Propag., vol.57, no.10, Oct. 2009.
[18] D.T. Le and Y. Karasawa, "A simple broadband antenna for MIMO applications in cognitive radio," IEICE Trans. Commun., vol.E95-B, no.1, pp.18–26, Jan. 2012.
[19] D.T. Le and Y. Karasawa, "A novel compact ultra-wideband dipole antenna," Proc. 6th European Conf. on Ant. and Prop. (EUCAP2012), Republic of Czech, March 2012.
[20] D.T. Le and Y. Karasawa, "Design of a broadband reconfigurable antenna for cognitive radio," Proc. IEEE Int. Ant. Propag. Symp., Chicago, July 2012.
[21] M. Rivera, J. Costantine, Y. Tawk, and C.G. Christodoulou, "Failure detection and correction in switch frequency reconfigurable antenna arrays," Proc. IEEE Ant. Propag. Symp., Washington, July 2011.
[22] M.J. Rivera, J. Costantine, Y. Tawk, and C.G. Christodoulou, "Detection of failures in switch reconfigurable antenna arrays using embedded sensing lines," Proc. IEEE Ant. Propag. Symp., Chicago, July 2012.

Dinh Thanh Le received B.S. and M.S. in Electronic Engineering from Le Quy Don Technical University (LQDTU), Ha Noi, Viet Nam, in 2006 and 2008, respectively. He completed a Ph.D. program in Electronics Engineering in The University of Electro-Communications (UEC), Tokyo, Japan in March 2012. From 2006 to 2008, he worked as a teaching assistant of LQDTU. Since May, 2012, he is an expert researcher at Electromagnetic Compatibility Laboratory, National Institute of Information and Communications Technology (NICT), Japan. His research interests include the topics of bio-electromagnetics, SAR measurement techniques, designs of MIMO antennas, broadband antennas, reconfigurable antennas, and microwaves. Dr. Le was the recipient research activities award from UEC in 2012. He also received best paper award in 2012 TriSAI conference, young scientist excellent paper award in the 2012 Pan-Pacific EMC Joint Meeting (PPEMC'12) organized by EMCJ, Japan, and student paper competition honorable mention in the 2011 IEEE APS Symposium.

Nguyen Quoc Dinh received the B.E., M.E. and D.E. degrees in Department of Electrical & Electonic Engineering, National Defense Academy, Yokosuka, Japan, in 2006, 2008, and 2011, respectively. Since 2011, he has been a Research Associate at the Department of Fundamentals of Radio and Electronic Engineering, Le Quy Don Technical University, Hanoi, Vietnam. His research interests include very small antennas, UWB antennas, MIMO antennas. He is a member of the Institute of Electronics, Information and Communication Engineers (IEICE), Japan. He was the recipient of the Young Scientist Award of the IEICE Antennas and Propagation Society Japan Chapter, Japan (2011).

Yoshio Karasawa received B.E. degree from Yamanashi University in 1973 and M.E. and Dr. Eng. Degrees from Kyoto University in 1977 and 1992, respectively. He joined KDD R&D Labs. in 1977. From July 1993 to July 1997, he was a Department Head of ATR Optical and Radio Communications Res. Labs. and ATR Adaptive Communications Res. Labs. both in Kyoto. Currently, he is a professor in the University of Electro-Communications (UEC), Tokyo, and a core member of Advanced Wireless Communication research Center (AWCC) in UEC. Since 1977, he has engaged in studies on wave propagation and antennas, particularly on theoretical analysis and measurements for wave-propagation phenomena, such as multipath fading in mobile radio systems, tropospheric and ionospheric scintillation, and rain attenuation. His recent interests are in frontier regions bridging "wave propagation" and "digital transmission characteristics" in wideband mobile radio systems such as MIMO. Dr. Karasawa received the Young Engineer Award from IECE of Japan in 1983, the Meritorious Award on Radio from the Association of Radio Industries and Businesses (ARIB, Japan) in 1998, Research Award from ICF in 2006, two Paper Awards from IEICE in 2006, and Best Tutorial Paper Awards in 2007 and 2008 from ComSoc of IEICE. He is a fellow of the IEEE.